Polymerization in Biozeolites

DOI: 10.1002/anie.201204178

Porous Dipeptide Crystals as Polymerization Nanoreactors**

*Gaetano Distefano, Angiolina Comotti, Silvia Bracco, Mario Beretta, and Piero Sozzani**

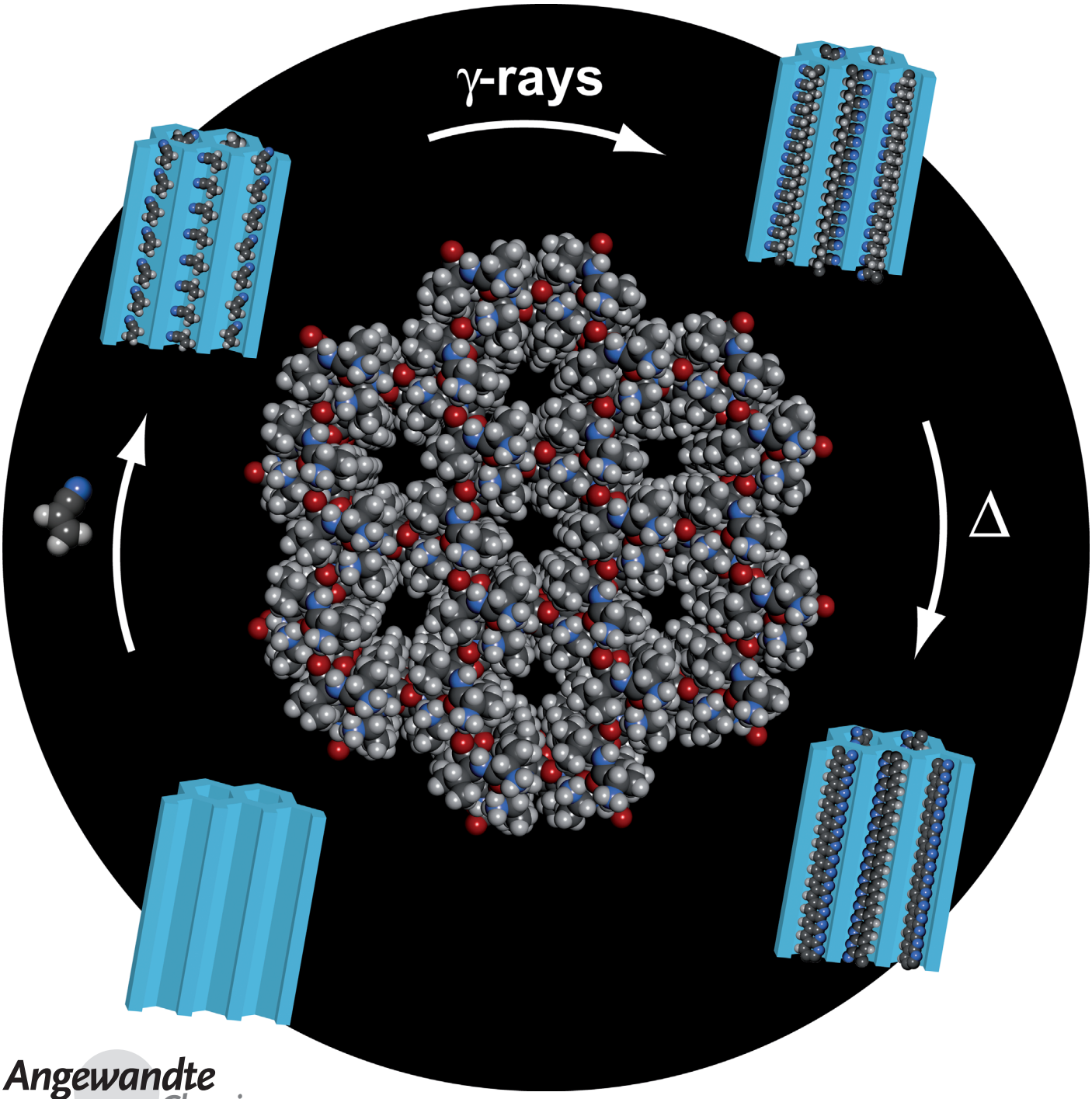

Peptides are fundamental constituents of living matter and are ubiquitous even in the simplest forms of life. They represent the first link between prebiotic and biotic substances and exhibit an extraordinary versatility in the fundamental functions of living organisms.[1] Peptides are being used, in both their natural and semi-synthetic forms, as an aid in the synthesis and implementation of novel functional molecular devices, such as nanowires, nanofibers, biohybrids, and biomachines.[2] The results collected to date indicate the enormous potential of these molecules for development in chemical applications.

The simplest class of peptides is dipeptides, which represent the first step of amino acid condensation. A number of them are uniquely endowed with structural voids in their crystalline structures, which have proven to be useful for gas diffusion and gas storage.[3] Dipeptides formed by L-alanine, L-valine, and L-isoleucine, hydrophobic amino acids, generate an isostructural ($P6_1$) series of porous crystals whose lattice is sustained by a recurrent charge-assisted hydrogen-bonding motif. These compounds contain aliphatic, one-dimensional nanochannels that have developed the topology of homochiral helices of diverse size and pitch (Figure 1).

Such spaces are potentially suitable as reaction vessels, and could be used for unconventional polymerizations within the peptide crystals. Indeed, polymer formation is a systematic process in biological organisms, and nature uses it to synthesize macromolecules for information storage, replication, and the fine control of 3D protein organization.[4] In this respect, porous dipeptide crystals, with cavities that can organize monomer arrangement, can function like enzymes, which impose steric constraints on the reactive substrates to produce controlled reactions.[5] Although the nanochannels in dipeptide crystals seem properly shaped for monomer inclusion and polymerization, such biocrystals have never, to our knowledge, been used as organized polymerization nanoreactors, in which crystalline order can be transcribed onto the polymer microstructure.[6] We explored the feasibility of artificial polymerization within the porous dipeptide crystals, and now report the first in situ γ-ray-induced solid-state polymerization of acrylic and diene monomers in crystals of naturally occurring dipeptides. Acrylonitrile, pentadiene, and isoprene were used as monomers in the porous crystals of L-alanyl-L-valine (Ala-Val), L-valyl-L-alanine (Val-Ala), L-isoleucyl-L-valine (Ile-Val), and L-valyl-L-isoleucine (Val-Ile), which have channels with diameters of 5.0, 4.7, 3.9 and 3.7 Å, respectively.[3a] Gamma-ray-induced polymerization led to the construction of regular polymers and their crystalline nanostructured adducts. Moreover, native poly(acrylonitrile) (PAN) chains extended in nanochannels can undergo intermolecular cyclization to ladder polymers and, eventually, be graphitized to yield carbon fibers. Because of the facile removal of the dipeptide crystal scaffold by vaporization or dissolution in water, the polymer fibrils are generated as replicas of the pristine crystals, enabling control over the polymer structure at the higher hierarchical level of morphology.[7]

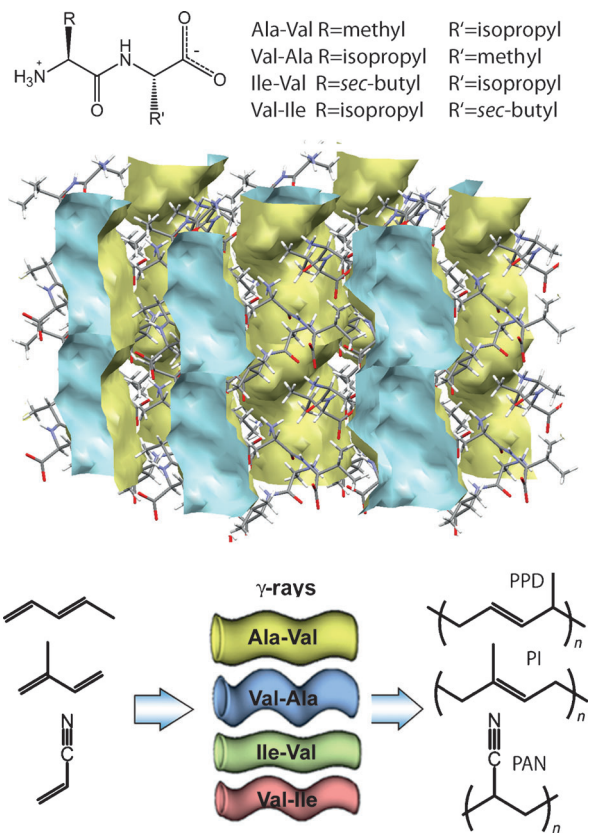

Figure 1. a) Chemical formula of the dipeptides. b) Crystal structure of porous Ala-Val compound showing the empty channels along the *c*-axis in blue and yellow. c) Schematic representation of the monomers and dipeptides used for the polymerization process.

Dipeptide crystal/monomer adducts were prepared by absorbing the monomer from the vapor phase on previously evacuated microporous samples. The driving force for the absorption was the stability of inclusion compounds formed spontaneously at the vapor pressure of the pure monomers.[8] The highly-penetrating, ionizing γ-ray radiation (^{60}Co source) generated the initiating radicals to promote polymerization. Such penetrating γ-rays offer the advantage of a homogeneous distribution of radical generation, and avoid the formation of by-products from chemical initiators. After irradiation, the sealed samples were left to polymerize for at least a week at room temperature, yielding dipeptide crystal/polymer adducts.

The dipeptide crystal/polymer adducts preserve their crystallinity, giving a hexagonal structure (space group $P6_1$) with XRD reflections as sharp as the pure porous dipeptide

[*] Dr. G. Distefano, Prof. A. Comotti, Dr. S. Bracco, Dr. M. Beretta, Prof. P. Sozzani
Department of Materials Science
University of Milano Bicocca
Via R. Cozzi 53, 20125 Milano (Italy)
E-mail: piero.sozzani@mater.unimib.it
Homepage: http://www.mater.unimib.it/utenti/sozzani/

[**] We thank Regione Lombardia and MIUR for financial support. Thanks to Dr. Martino Mauri for technical support and Prof. A. Faucitano for access to irradiation facilities.

Supporting information for this article (experimental details) is available on the WWW under http://dx.doi.org/10.1002/anie.201204178.

crystals, indicating that upon monomer sorption, irradiation, and polymerization the entire structure undergoes no dramatic changes (Figure 2). Powder X-ray diffraction patterns of the dipeptide crystal/polymer adducts compared to the pristine porous dipeptide crystals indicate a slight unit-cell-volume increase upon in situ polymer formation, as evaluated by refinement of the XRD patterns: the *a*- and *b*-axes expand to accommodate the guest polymer while the *c*-axis shrinks slightly (see Supporting Information).

Thermogravimetric analyses, performed under non-oxidative conditions, enabled us to quantitatively evaluate the guest content of each adduct. The pure dipeptide crystals showed no mass residue above 300 °C while dipeptide crystal/polymer adducts exhibited a mass residue, by which we could determine the polymer content. In the case of the Ala-Val/poly(acrylonitrile) compound (Ala-Val/PAN), assuming a monomer unit repeat distance of 2.5 Å for the PAN chain in the stretched conformation and the structural parameters of the dipeptide channels, we could calculate a pore filling of 90 %. High yields of PAN, close to complete channel loading, were also achieved in the narrower Val-Ile crystal channels. Moreover, the isoprene monomer polymerized at high yields in the larger pores of Ala-Val and Val-Ala (about 80 % pore filling).

SEM micrographs showed, after polymerization, morphologically unaltered crystals with neat edges, indicative of the absence of polymerization on the crystal surfaces or in the intercrystalline spaces (see Supporting Information). The occurrence of polymerization exclusively within the crystal channels is shown by the absence of a glass transition or polymer melting in the differential scanning calorimetry (DSC) scans.[9]

The molecular weight of the polymers after dissolution of the peptide crystal in water ranges from 50 to 150 kDa (Mark–Houwink parameter: $K = 0.032\ \mathrm{mL\,g^{-1}}$ and $a = 0.75$) for PAN, from 20 to over 68 kDa for poly(pentadiene) (PPD), and from 100 to 156 kDa for poly(isoprene) (PI; masses from gel permeation chromatography (GPC) in tetrahydrofuran (THF)). The high molecular mass of the resulting polymers suggests that the propagating radicals are long lived, and promote the polymerization over a large number of monomer units. Insight into the polymer microstructure was obtained by ^{1}H and ^{13}C solution NMR spectroscopy. The ^{13}C NMR spectra of PPD polymerized in Ala-Val (Figure 3a) featured the characteristic signals of the 1,4-*trans* polymer without regiochemical errors or pendant vinyl groups.[10]

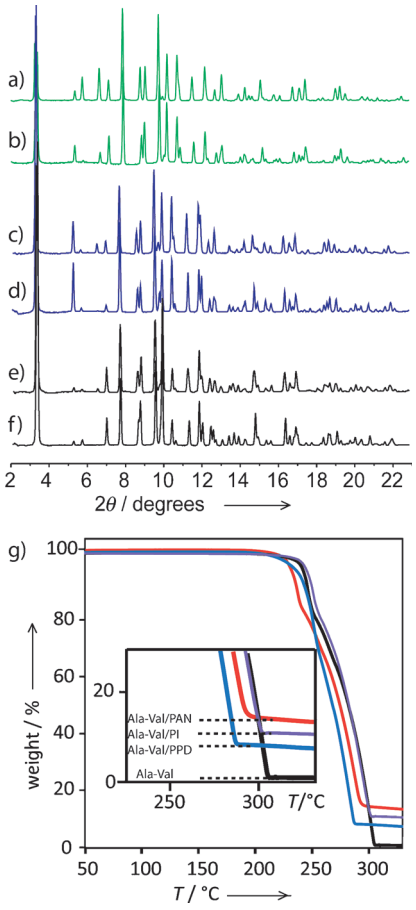

Figure 2. Synchrotron-source powder X-ray diffraction patterns of Ala-Val/PAN, Ile-Val/PAN, Val-Ile/PAN nanocomposites (a, c, e) and porous Ala-Val, Ile-Val, Val-Ile crystals (b, d, f). g) Thermogravimetric traces of the three Ala-Val nanocomposites with respect to the pure dipeptide.

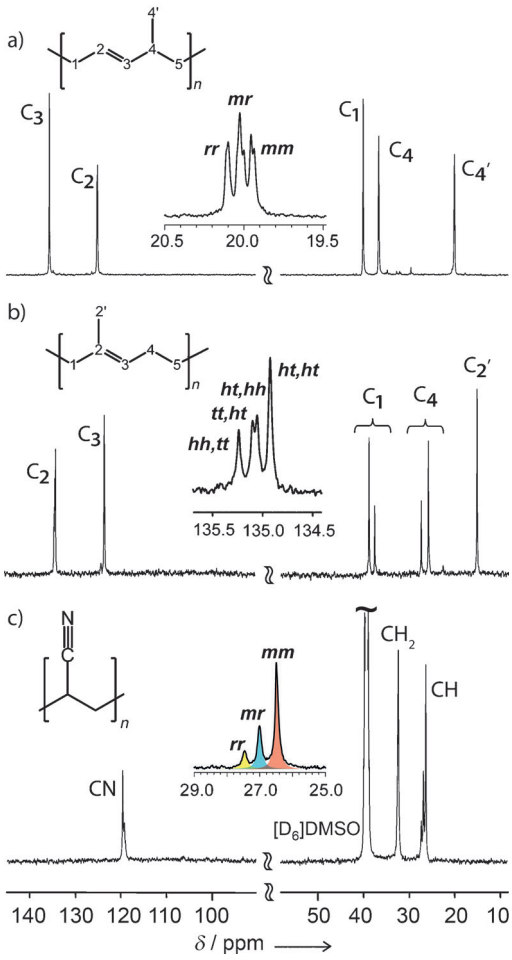

Figure 3. ^{13}C solution NMR spectra of a) 1,4-*trans*-poly(pentadiene), b) 1,4-*trans*-poly(isoprene), and c) isotactic PAN, as extracted from Ala-Val/polymer nanocomposites.

The formation of a linear 1,4-*trans* polymer is the fingerprint of in-channel polymerization because the confinement to channels makes bulkier monomer-unit configurations (1,4-*cis* and 1,2-) sterically forbidden, thus selectively yielding the polymer with the best fitting configuration for a channel cross-section of about 5 Å. Further expansion of the methyl region of the NMR spectrum enables the elucidation of polymer stereochemistry. The CH_3 signal split into three peaks, each assigned at the triad level: $\delta_C = 19.96$ ppm (isotactic, *mm*), 20.00–20.05 ppm (heterotactic, *mr* and *rm*), and 20.11 ppm (syndiotactic, *rr*). Peak simulation demonstrates Bernoullian statistics with relative peak integrals in a 1:2:1 ratio. Similar results were obtained for polymerization in Ile-Val and Val-Ile microporous systems (see Supporting Information), demonstrating the general behavior of topochemical polymerization in such biological materials.

Isoprene polymerization was undertaken with the aim of synthesizing 1,4-*trans*-poly(isoprene), produced naturally by plants using enzymatic synthesis.[11] Figure 3b shows the ^{13}C NMR spectrum of PI obtained in Ala-Val nanochannels. The main five resonances show repeat units containing five carbon atoms in a regular head-to-tail 1,4-*trans* configuration. A more detailed analysis of the methylene region ($\delta_C = 27$ and 40 ppm) can be interpreted at the dyad level, and highlights the presence of minor amounts of head-to-head *hh* and tail-to-tail *tt* linkages, although the stereoregular 1,4-*trans* structure persists. The enlargement of the region at about 135 ppm (C_2) shows a fine structure that is sensitive to monomer unit triads. The signal intensity distribution with 1:1:1 ratio for *hh*,*tt tt*,*ht ht*,*hh* sequences, shows that the growing chain has the occasional inversion of a single monomer unit; after this inversion, chain regularity is immediately restored.[12] This behavior is comparable to that of coordination polymerization when catalyst control prevails over chain control, suggesting an analogy between biocrystal pores and catalytic sites.

^{13}C NMR spectra of the poly(acrylonitrile) freed from crystal matrices exhibited three signal groups associated with three carbon nuclei, revealing a regular head-to-tail addition without regiodefects (Figure 3c). Each of the signals of the ^{13}C NMR spectra showed a fine structure. Methine signals were used to estimate polymer stereoregularity, showing that the PAN polymerized in the narrow pores of Ile-Val and Val-Ile crystals is atactic while the polymer synthesized in the large Ala-Val pores is isotactic with an *m* diad content of 78%.[13] From the triad distribution, details of chain stereochemistry can be inferred. In principle, two models can be considered: a single sindiotactic dyad *r* inserted in an extended isotactic sequence, or *rr* triads cast in an isotactic sequence (see Supporting Information). The second model is consistent with our data (*mm* = 61, *mr* = 27, and *rr* = 12), where a single CN group constitutes an isolated configurational defect in a long stereocontrolled isotactic chain. This result suggests that a self-correction mechanism, owing to steric constraints imposed by the crystal, was effective during the polymerization. Isotactic PAN cannot be obtained by conventional polymerization methods, the only exception being polymerization in urea, performed at low temperature because of the instability of the urea/acrylonitrile adduct above −25 °C.[6k] In the present case we achieved isotactic PAN at room temperature, thanks to the remarkable monomer absorption of our "biozeolites" under mild conditions of temperature and pressure.

A notable advantage of using dipeptides in the zwitterionic form is their rapid dissolution in water at room temperature, allowing morphological features of the crystal to be preserved in the polymer. Indeed, polymer fibrils were obtained in a few minutes by the selective matrix dissolution of the Ala-Val/PAN nanocomposite, as highlighted by in situ optical microscopy (see Supporting Information). For comparison purposes, the complete dissolution of pure Ala-Val crystals is also reported. The synthesized poly(acrylonitrile) fibrils retain the length and aspect-ratio of the original crystalline nanocomposites, although the polymeric material can develop a curvature. These fibrils were characterized by NMR spectroscopy and DSC, and proved to be pure polymers, completely free of dipeptide molecules.

Moreover, porous dipeptide crystals permitted post-modification reactions to be carried out on polymers confined in their nanochannels. Specifically, PAN was transformed into a polyconjugated ladder polymer by high-temperature thermal intramolecular cyclization involving a nitrile group chain reaction. PAN macromolecules, encapsulated in the nanochannels as extended chains, are assisted during transformation to the ladder polymer by the supramolecular peptidic scaffold (Figure 4). During thermal treatment the matrix was easily removed because the dipeptides are vaporized at 270–320 °C, thus the polymer ladder was freed from the sacrificial peptidic scaffold without chemical treatment. The formation of a ribbon of condensed cyclic structures results in polymer chains with markedly reduced conformational flexibility, thus further thermal treatment of the rigid chain at 1100 °C under inert atmosphere, produced graphitic micro-objects retaining the original aspect ratio and shape of the dipeptide crystals (Figure 4).[14]

SEM images of the thermally processed adducts showed that the crystals preserved the needle-like shape, without collapsing or substantial bending. Statistical analysis of morphological parameters based on SEM micrographs of samples at various treatment stages showed that the distribution of needle length did not change (see Supporting

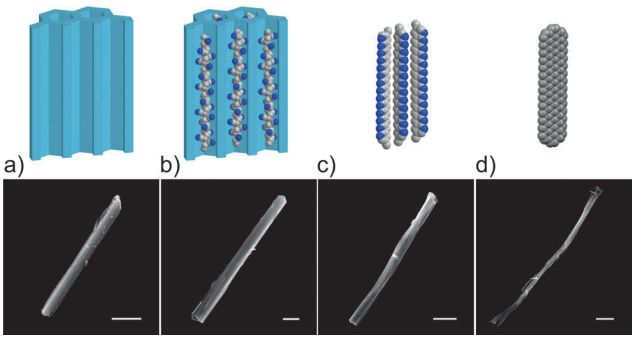

Figure 4. SEM images of a) an individual Ala-Val crystal, b) Ala-Val/PAN crystalline adduct, c) ladder-polymer fibril after removal of the crystal, and d) graphitized carbon fibril. Scale bar = 20 μm. Schematic representation of the process at the molecular level is shown above.

Information), while the width became smaller (average thickness changed from 3.1 ± 1.0 μm for pure Ala-Val crystals to 1.6 ± 0.9 μm for carbonized fibrils); this indicates matrix removal and lateral interchain association upon thermal treatment. Raman spectroscopy confirmed the graphitic nature of the fibrils with a consistent *G*/*D* band ratio, and a line width typical of carbon fibers from graphitized poly(acrylonitrile) (see Supporting Information).[14] The PAN synthesis and subsequent curing in dipeptide crystals suggests an unusual way to produce stretched graphitic carbon fibrils by alignment of the parent PAN in crystalline nanochannels of that are biological in origin.

In conclusion, we have demonstrated the possible use of porous dipeptide crystals ("biozeolites") containing channels of distinct cross-sections as nanoreactors for topochemical polymerizations. The diene polymers exclusively exhibited a 1,4-*trans* configuration, while control over tacticity was achieved in poly(acrylonitrile) grown in the channels, producing an isotactic polymer at room temperature. The possibility of transferring the exquisite order and versatility of porous biological crystals to synthetic polymer structures opens up new opportunities for reactions in biological media. This achievement could be useful to current efforts to use biological molecules for synthetic purposes. Specifically, the unconventional use of sacrificial peptide crystals for the preparation of synthetic polymers offers intriguing opportunities for chemists to design controlled reactions in the solid state.

Received: May 29, 2012
Published online: August 15, 2012

Keywords: crystal engineering · microporous materials · peptides · polymerization · topochemistry

[1] N. Swald, H.-D. Jakube, *Peptides: Chemistry and Biology*, Wiley-VCH, Weinheim, **2009**.

[2] a) J. S. Lee, I. Yoon, J. Kim, H. Ihee, B. Kim, C. B. Park, *Angew. Chem.* **2011**, *123*, 1196 – 1199; *Angew. Chem. Int. Ed.* **2011**, *50*, 1164 – 1167; b) M. C. McAlpine, H. D. Agnew, R. D. Rohde, M. Blanco, H. Ahmad, A. D. Stuparu, W. A. Goddard, J. R. Heath, *J. Am. Chem. Soc.* **2008**, *130*, 9583 – 9589; c) J. B. Matson, R. H. Zha, S. I. Stupp, *Curr. Opin. Solid State Mater. Sci.* **2011**, *15*, 225 – 235; d) L. Adler-Abramovich, N. Kol, I. Yanai, D. Barlam, R. Z. Shneck, E. Gazit, R. Ehud, *Angew. Chem.* **2010**, *122*, 10135 – 10138; *Angew. Chem. Int. Ed.* **2010**, *49*, 9939 – 9942; e) C.-L. Chen, P. Zhang, N. L. Rosi, *J. Am. Chem. Soc.* **2008**, *130*, 13555 – 13557; f) L. Adler-Abramovich, D. Aronov, P. Beker, M. Yevnin, S. Stempler, L. Buzhansky, G. Roseman, E. Gazit, *Nat. Nanotechnol.* **2009**, *4*, 849 – 854; g) C.-L. Chen, N. L. Rosi, *Angew. Chem.* **2010**, *122*, 1968 – 1986; *Angew. Chem. Int. Ed.* **2010**, *49*, 1924 – 1942; h) C. Li, J. Adamcik, R. Mezzenga, *Nat. Nanotechnol.* **2012**, *7*, 421 – 427; i) M.-J. Teng, X.-R. Jia, X.-F. Chen, Y. Wei, *Angew. Chem.* **2012**, *124*, 6504 – 6507; *Angew. Chem. Int. Ed.* **2012**, *51*, 6398 – 6401; j) J. Rabone, Y. F. Yue, S. Y. Chong, K. C. Stylianou, J. Bacsa, D. Bradshaw, G. R. Dalring, N. G. Berry, Y. Z. Khimyak, A. Y. Ganin, P. Wiper, J. B. Claridge, M. J. Rosseinsky, *Science* **2010**, *329*, 1053 – 1057.

[3] a) C. H. Görbitz, *Chem. Eur. J.* **2007**, *13*, 1022 – 1031; b) C. H. Görbitz, *New J. Chem.* **2003**, *27*, 1789 – 1793; c) D. V. Soldatov, I. L. Moudrakovski, E. V. Grachev, J. A. Ripmeester, *J. Am. Chem. Soc.* **2006**, *128*, 6737 – 6744; d) A. Comotti, S. Bracco, G. Distefano, P. Sozzani, *Chem. Commun.* **2009**, 284 – 286; e) C. H. Görbitz, *CrystEngComm* **2005**, *7*, 670 – 673; f) C. H. Görbitz, M. Nilsen, K. Szeto, L. W. Tangen, *Chem. Commun.* **2005**, 4288 – 4290; g) I. Moudrakosvski, D. V. Soldatov, J. A. Ripmeester, D. N. Sears, C. J. Jameson, *Proc. Natl. Acad. Sci. USA* **2004**, *101*, 17924 – 17929; h) S. Guha, T. Chakraborty, A. Banerjee, *Green Chem.* **2009**, *11*, 1139 – 1145; i) S. Guha, M. G. B. Drew, A. Banerjee, *Chem. Mater.* **2008**, *20*, 2282 – 2290.

[4] a) U. Hübscher, G. Maga, S. Spadari, *Annu. Rev. Biochem.* **2002**, *71*, 133 – 163; b) J. Hurwitz, *J. Biol. Chem.* **2005**, *280*, 42477 – 42485; c) K. B. Mullis, *Angew. Chem.* **1994**, *106*, 1271 – 1276; *Angew. Chem. Int. Ed. Engl.* **1994**, *33*, 1209 – 1213; d) H. Lodish, A. Berk, S. L. Zipursky, P. Matsudaira, D. Baltimore, J. Darnell, *Molecular Cell Biology*, W. H. Freeman, New York, **2000**.

[5] a) L. Loss, *Biocatalysis in Polymer Chemistry*, Wiley-VCH, Weinheim, **2010**; b) S. Kundu, A. S. Bhangale, W. E. Wallace, K. M. Flynn, C. M. Guttman, R. A. Gross, K. L. Beers, *J. Am. Chem. Soc.* **2011**, *133*, 6006 – 6011; c) R. A. Gross, A. Kumar, B. Kalra, *Chem. Rev.* **2001**, *101*, 2097 – 2124.

[6] a) T. Uemura, N. Yanai, S. Kitagawa, *Chem. Soc. Rev.* **2009**, *38*, 1228 – 1236; b) T. Uemura, S. Horike, K. Kitagawa, M. Mizuno, K. Endo, S. Bracco, A. Comotti, P. Sozzani, M. Nagaoka, S. Kitagawa, *J. Am. Chem. Soc.* **2008**, *130*, 6781 – 6788; c) K. Kageyama, J.-I. Tamazawa, T. Aida, *Science* **1999**, *285*, 2113 – 2115; d) P. Enzel, T. Bein, *Chem. Mater.* **1992**, *4*, 819 – 824; e) M. Farina, G. Di Silvestro, P. Sozzani in *Comprehensive Supramolecular Chemistry*, *Vol. 6* (Ed.: J.-M. Lehn), Pergamon, Oxford, **1996**, pp. 371 – 398; f) K. Tajima, T. Aida, *Chem. Commun.* **2000**, 2399 – 2412; g) Y. Lu, Y. Yang, A. Sellinger, M. Lu, J. Huang, H. Fan, R. Haddad, G. Lopez, A. R. Burns, D. Y. Sasaki, J. Shelnutt, C. J. Brinker, *Nature* **2001**, *410*, 913 – 917; h) M. Miyata, K. Sada in *Comprehensive Supramolecular Chemistry*, *Vol. 6* (Ed.: J.-M. Lehn), Pergamon, Oxford, **1996**, pp. 147 – 176; i) M. Farina, G. Di Silvestro, P. Sozzani, *Macromolecules* **1985**, *18*, 923 – 928; j) H. R. Allcock, E. N. Silverberg, G. K. Dudley, S. R. Pucher, *Macromolecules* **1994**, *27*, 7550 – 7555; k) M. Minagawa, H. Yamada, K. Yamaguchi, F. Yoshi, *Macromolecules* **1992**, *25*, 503 – 510.

[7] a) B. H. Jones, T. P. Lodge, *ACS Nano* **2011**, *5*, 8914 – 8927; b) P. Sozzani, S. Bracco, A. Comotti, R. Simonutti, P. Valsesia, Y. Sakamoto, O. Terasaki, *Nat. Mater.* **2006**, *5*, 545 – 550; c) N. Yanai, T. Uemura, M. Ohba, Y. Kadowaki, M. Maesato, M. Takenaka, S. Nishitsuji, H. Hasegawa, S. Kitagawa *Angew. Chem.* **2008**, *120, 10031 – 10034; Angew. Chem. Int. Ed.* **2008**, 47, 9883 – 9886; *Angew. Chem. Int. Ed.* **2008**, *47*, 9883 – 9886; d) M. Choi, R. Ryoo, *Nat. Mater.* **2003**, *2*, 473 – 476; e) S. Kazuki, T. Masayuki, F. Norifumi, M. Numata, S. Shinkai, *Chem. Soc. Rev.* **2007**, *36*, 415 – 435; f) S. A. Johnson, P. J. Ollivier, T. E. Mallouk, *Science* **1999**, *283*, 963 – 965.

[8] Adsorption isotherms demonstrated that dipeptide crystals can absorb linear alkane vapors until complete filling of the pores at room temperature (see Supporting Information).

[9] a) P. Sozzani, S. Bracco, A. Comotti, R. Simonutti, *Adv. Polym. Sci.* **2005**, *181*, 153 – 177; b) R. Krishnamoorti, R. A. Vaia, E. P. Giannelis, *Chem. Mater.* **1996**, *8*, 1728 – 1734.

[10] P. Sozzani, G. Di Silvestro, M. Grassi, M. Farina, *Macromolecules* **1984**, *17*, 2532 – 2538.

[11] J. E. Puskas, E. Gautriaud, A. Deffieux, J. P. Kennedy, *Prog. Polym. Sci.* **2006**, *31*, 533 – 548.

[12] a) G. Di Silvestro, P. Sozzani, M. Farina, *Macromolecules* **1987**, *20*, 999 – 1003; b) F. C. Schilling, P. Sozzani, F. A. Bovey, *Macromolecules* **1991**, *24*, 4369 – 4375.

[13] F. A. Bovey, P. A. Mirau, *NMR of Polymers*, Academic Press, San Diego, **1996**.

[14] a) E. Fitzer, *Carbon* **1989**, *27*, 621 – 645; b) T. H. Ko, *J. Appl. Polym. Sci.* **1996**, *59*, 577 – 580.

